Novel Electrochemical Sensing Platform Based on a Molecularly Imprinted Polymer Decorated 3D Nanoporous Nickel Skeleton for Ultrasensitive and Selective Determination of Metronidazole

Yingchun Li,*[†,‡] Yuan Liu,[†] Yang Yang,[†] Feng Yu,[‡] Jie Liu,[†] Han Song,[†] Jiang Liu,[†] Hui Tang,[†] Bang-Ce Ye,[‡] and Zhipeng Sun*[§]

[†]Key Laboratory of Xinjiang Endemic Phytomedicine Resources, Ministry of Education, School of Pharmacy, Shihezi University, Shihezi 832002, China

[‡]Key Laboratory for Green Processing of Chemical Engineering of Xinjiang Bingtuan, School of Chemistry and Chemical Engineering, Shihezi University, Shihezi 832003, China

[§]Xinjiang Uygur Autonomous Region Product Quality Supervision and Inspection Institute, Urumqi 830011, China

S *Supporting Information*

ABSTRACT: A novel electrochemical sensor has been developed by using a composite element of three-dimensional (3D) nanoporous nickel (NPNi) and molecularly imprinted polymer (MIP). NPNi is introduced in order to enhance the electron-transport ability and surface area of the sensor, while the electro-synthesized MIP layer affords simultaneous identification and quantification of the target molecule by employing $Fe(CN)_6^{3-/4-}$ as the probe to indicate the current intensity. The morphology of the hybrid film was observed by scanning electron microscopy, and the properties of the sensor were examined by cyclic voltammetry and electrochemical impedance spectroscopy. By using metronidazole (MNZ) as a model analyte, the sensor based on the MIP/NPNi hybrid exhibits great features such as a remarkably low detection limit of 2×10^{-14} M (S/N = 3), superb selectivity in discriminating MNZ from its structural analogues, and good antiinterference ability toward several coexisting substances. Moreover, the proposed method also demonstrates excellent repeatability and stability, with relative standard deviations of less than 1.12% and 1.4%, respectively. Analysis of MNZ in pharmaceutical dosage form and fish tissue is successfully carried out without assistance of complicated pretreatment. The MIP/NPNi composite presented here with admirable merits makes it a promising candidate for developing electrochemical sensor devices and plays a role in widespread fields.

KEYWORDS: electrochemical sensor, molecularly imprinted polymer, nanoporous nickel, metronidazole, trace level measurement
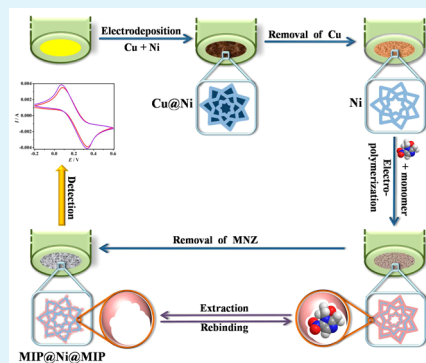
1. INTRODUCTION

Metronidazole (MNZ) is a nitroimidazole derivative and has been widely applied in human beings, animals, and fish for curing protozoal and bacterial diseases.[1−3] In addition, it is also used as a promoter to induce the growth of aquatic products.[4,5] However, because MNZ shows genotoxic, carcinogenic, and mutagenic side effects,[6,7] its application in aquaculture and farming industries has been prohibited by many countries and areas.[8,9] Thus, the accurate determination of trace levels of MNZ is necessary in various samples. Different methods have been reported for detecting MNZ, such as spectrophotometry,[10,11] thin-layer chromatography,[12] gas chromatography,[13] high-performance liquid chromatography (HPLC),[14] and electrochemistry.[5,7,15−25] Some of these strategies suffer from disadvantages including the involvement of time-consuming manipulation steps, requirement of sophisticated equipment and skilled operators, consumption of a large amount of organic reagent, etc.[26,27] Among them, an electroanalytical sensing technique has been proven to be an attractive route owing to its high sensitivity, simplicity, rapid analysis period, and low-cost apparatus.[5,7,15−25]

As a key component in the sensor system, the sensing agent has drawn numerous attempts both in material itself and in modification strategy. Among multifarious approaches, the molecular imprinting technique,[28−30] which could produce a polymeric network owning specific binding sites, has become a powerful tool for the preparation of sensitive agents with a predetermined recognition capacity for chem/biospecies of interest. The principle of preparing a molecularly imprinted polymer (MIP) involves polymerization of a functional monomer in the presence of a template molecule and subsequent template extraction from the polymer network,

leaving sites with induced molecular memory that are capable of recognizing the previously imprinted molecules.[31,32] A promising method to synthesize MIP on an electrode surface is in situ electropolymerization, by which a polymeric layer can easily grow directly on an electrode of any shape, and its thickness is controlled by adjusting the synthesis conditions like the amount of monomer, circulated charge, etc.[30,33,34] This strategy is highly controllable and flexible, allowing for a fast sensing response, miniaturization of the sensor architecture, and reproducibility of sensor manufacture.

On the other hand, high sensitivity and detection capacity are other common requirements in the sensor industry, and it is easy to understand that a three-dimensional (3D) porous surface is superior to a flat electrode because the former can not only provide a highly conductive framework for electron transfer but also possess a hierarchical porous structure and high surface area favoring fast electrolyte diffusion and facile faradic reaction. Thus, materials including metals (Al, Au, etc.),[18,35] carbons,[36] oxides (SnO_2),[37] and nitrides[38] with nanoscale and porous features have been extensively applied to modify planar electrodes. However, most of the modification processes such as drop coating, physical adhesion, etc., often lead to the decoration falling off easily under liquid conditions, and consequently the fabricated sensors suffer from instability and poor reproducibility. Hence, it is of primary importance to develop an alternative decorating method. Electrodeposition of the metal layer onto the electrode surface has been employed as a unique modifying method because of controlled operation, sturdy construction, and stability.[39] When it comes to the constituent of a 3D nanoporous agent, noble metals have been reported,[40,41] but rising cost is the main hindrance toward their large-scale practical application. Accordingly, effort has been put into adopting low-cost material with comparably high electronic property, and metals (Ni and Cu)[42−44] and metal oxides (CuO, Co_3O_4, and NiO)[45−48] have shown excellent performance in the aspect of electron transfer. Therefore, it is expected that a 3D nanoporous nickel (NPNi) structure should serve as an ideal electrode architecture for loading other sensing material. To the best of our knowledge, this point has not been addressed before in the field of sensors.

In this article, a hybrid sensing platform based on composite elements consisting of NPNi covered by an ultrathin MIP film has been constructed for the first time. Both layers were synthesized by a highly controlled electrodeposition process, ensuring the stability and reproducibility of the resultant sensor. The sensor performance was evaluated by using MNZ as a model analyte, which displayed superb sensitivity, selectivity, and a wide detection range. Furthermore, the novel sensor was successfully employed to recognize and detect MNZ in the pharmaceutical dosage form and real biological samples.

2. EXPERIMENT

2.1. Chemicals and Apparatuses. Metronidazole (MNZ), ronidazole, 4-nitroimidazole, 1,2-dimethylimidazole, dimetridazole, and o-phenylenediamine were purchased from Aladdin Co. (Shanghai, China). Nickel sulfate was obtained from Adamas Reagent Co. Ltd. (Shanghai, China). Copper sulfate and boric acid were supplied by Alfa Aesar Co. (Tianjin, China). MNZ tablets were obtained from a local drugstore. Crucian fish was obtained at a local market. Reagents and materials, such as starch, sucrose, dextrin glucose, $Fe(CN)_6^{3-/4-}$, $CaCl_2$, NH_4Cl, NaCl, KNO_3, KCl, H_2SO_4, HNO_3, methanol, and a phosphate buffer solution (KH_2PO_4 and K_2HPO_4) were of analytical grade and were used without further purification. Aqueous solutions were prepared with double-distilled water.

Electrochemical data were obtained by using a CHI 760E Electrochemical Workstation (CHI Instruments Co., Shanghai, China) connected to a personal computer at room temperature. A typical three-electrode system was employed with a platinum wire (0.5 mm in diameter and 34 mm in length) as the auxiliary electrode and a saturated calomel electrode (SCE) as the reference electrode, and the working electrode was a bare or modified planar gold electrode (GE; 4 mm in diameter). All potentials given in this paper referred to SCE. The surface morphology of NPNi was characterized with a Zeiss Supra55VP scanning electron microscope operating at 20 kV.
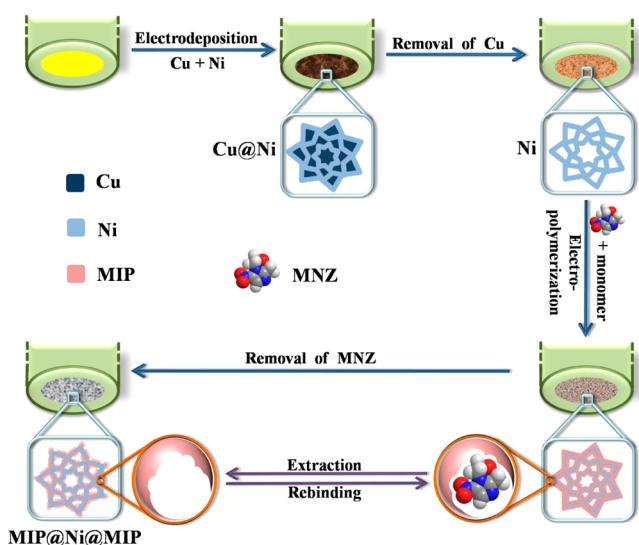
HPLC was performed using an Essentia LC-10A system equipped with an LC-10A Solvent Delivery Unit, an LC Solution 10A workstation, and an SPD-10A UV−vis detector (Shimadzu, Japan). LC condition was as follows: chromatographic separation was performed on a Shimadzu WondaSil C_{18} column (150 mm × 4.6 mm i.d., 5 μm). The mobile phase was methanol/water (2:8, v/v) with a flow rate of 1.0 mL min^{-1}, and the detection wavelength was set at 315 nm. A KQ 300 ultrasonic cleaner (Kunshan Instrument Co., Jiangsu, China) was set at 40 kHz. All measurements were performed in triplicate.

2.2. Preparation of MIP/NPNi/GE. A GE was polished carefully to a mirrorlike surface with a 0.3−0.05 μm alumina aqueous slurry, and then it was washed thoroughly with alcohol and distilled water. Before the experiment, the bare GE was cyclic-potential-scanned within the potential range of −0.2 to +0.6 V in a $Fe(CN)_6^{3-/4-}$ probe solution [containing 0.1 M KNO_3 and 0.1 M $Fe(CN)_6^{3-/4-}$] as the supporting electrolyte, until a pair of rather well-defined redox peaks was obtained.

The NPNi film was prepared as previously reported.[42] Briefly, a Ni−Cu alloy film was electrodeposited onto a bare GE in a three-electrode cell containing 1.0 M $NiSO_4$, 0.01 M $CuSO_4$, and 0.5 M H_3BO_3 (pH = 4). The film was deposited under a constant potential of −0.75 V, and the total cathodic passed charge was controlled at 0.4 C cm^{-2}. When the electrochemical system is supplied with the external voltage of −0.75 V, the working electrode acts as a cathode, where the metal ions of Cu^{2+} and Ni^{2+} in the electrolyte solution are reduced, such that they "plate out" into metal atoms on the cathode surface to form a Ni−Cu alloy. Selective dissolution of Cu from the deposited Ni−Cu film was then conducted in the same solution by applying a potential of +0.2 V. In this case, the working electrode acts as an anode, where oxidation of Cu to Cu^{2+} occurs, allowing them to dissolve in the solution. Because Ni is stable under a potential of +0.2 V, it remains as an atom on the electrode surface.[42] The developed NPNi electrode was denoted as NPNi/GE.

Electropolymerization of MIPs in the presence of MNZ on the NPNi/GE surface was realized by cyclic voltammetry (CV), which was implemented between 0 and +0.8 V for 150 consecutive cycles at a scan rate of 50 mV s^{-1} in a solution containing MNZ and o-phenylenediamine as a functional monomer. Then NPNi/GE bearing the polymer film was immersed in 0.1 M NaOH to extract embedded MNZ through magnetic stirring for 30 min and CV scanning between −0.5 and +0.5 V for several cycles until an evident redox peak could be observed in the probe solution again. The schematic representation for the preparation of MIP/NPNi/GE is illustrated in Figure 1. As a control, a nonimprinted polymer (NIP)-modified electrode was prepared and treated in exactly the same way except with omission of template molecules. Several parameters concerning the MIP preparation can be found in ref 23.

2.3. Electrochemical Measurement. The electrochemical sensor was immersed in a solution containing the desired concentration of the analyte for 10 min and carefully washed with distilled water to remove the physical adsorbed substances. After that, it was transferred to a three-electrode system assembled in a cell with a 0.1 M $Fe(CN)_6^{3-/4-}$ probe solution. Cyclic voltammograms were recorded between −0.2 and +0.6 V at a scan rate of 100 mV s^{-1}. A washing step was followed after detection of one kind of analyte to extract sorbed compounds, where the modified electrode was immersed in NaOH upon scanning between −0.5 and +0.5 V for several cycles until a stable redox peak could be observed. Preliminary studies on the electrochemical behavior of the modified electrodes were performed by CV and

Figure 1. Schematic representation for the preparation of MIP/NPNi/GE.

Figure 2. SEM micrographs of a Cu−Ni alloy (a), NPNi (b), MIP/NPNi before (c) and after (d) extraction of MNZ. EDS spectrograms of a Cu−Ni alloy (e) and NPNi (f).

electrochemical impedance spectra in the desired solution. All measurements were performed at room temperature.

2.4. Detection of a MNZ Tablet and MNZ in a Biological Sample. For the purpose of confirming the performance and feasibility of the modified sensor in monitoring the pharmaceutical product and complex matrix of real samples, MIP/NPNi/GE was applied to measure MNZ in tablet form and in fish meat. A total of 10 pieces of MNZ tablets (each containing 200 mg of MNZ) were accurately weighed, crushed, and mixed in a mortar. A portion of the powder equivalent to 250 mg of MNZ was dissolved with methanol, ultrasonicated for 5 min to allow complete dissolution of MNZ, and then filtered. The filtrate solution was diluted to a desired concentration with methanol for MNZ analysis. For the spiked recovery experiment, a certain amount of MNZ was added to the tablet powder. As for MNZ detection in fish meat, the experiment was carried out as follows. A healthy crucian carp fish fasted for 24 h and was fed a certain amount of MNZ mixed in fodder. After feeding for 48 h, 2.0 g of fish meat with fish skin and bones removed was homogenized with 7 mL of methanol. Thereafter, methanol was added to the homogenate at a volumetric ratio of 1:1 to get rid of protein, followed by centrifugation. The supernatants were used for MNZ detection. Likewise, for the spiked recovery experiment, a certain amount of MNZ was added in the samples during the homogenization process.

3. RESULTS AND DISCUSSION

3.1. Preparation and Characterization of MIP/NPNi/GE. The electropolymerization process of the MIP layer was characterized by CV, and typical scans are displayed in Figure S1 (Supporting Information, SI). As suggested by the prominent decrease of the current intensity under consecutive cyclic scans, an insulating polymeric film was formed, gradually covering the electrode surface and leading to restraint of the voltammetric response. The voltammograms (Figure S1 in the SI) show an electrochemically irreversible reaction.

The electrodes were first characterized by scanning electron microscopy (SEM), which displays a series of regular patterns on the surface of electrodes with different modifications. Figure 2a shows the solid starfish-like morphology of a Cu−Ni alloy modified electrode (∼500 nm in diameter). The atomic ratio of Cu and Ni is close to 1:1, as confirmed by energy-dispersive spectrometry (EDS) in Figure 2e. After removal of Cu from the alloy, the solid grains transformed into hollow flowerlike shapes
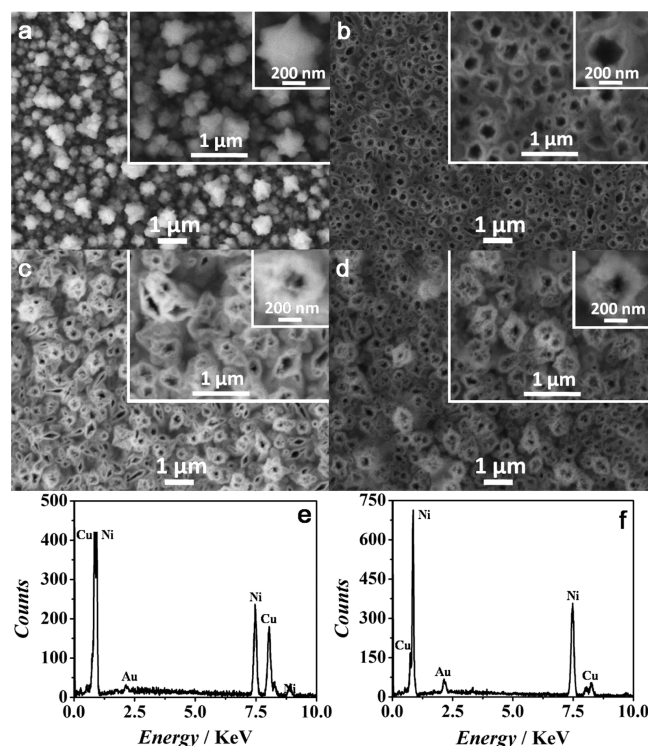
(Figure 2b) with nanopores (∼100−250 nm in diameter), while the ratio of Cu and Ni was investigated as 10:1 (Figure 2f), implying that Cu was almost completely removed. After further modification of the hollow Ni by electropolymerization of o-aminophenol in the presence of MNZ, the Ni wall obviously thickened (Figure 2c) along with a decrease in the size of the nanopores. When MNZ was extracted from the polymeric network, the Ni walls became thinner and coarser and the nanopores got larger (Figure 2d).

The electrochemical behavior for the stepwise fabrication procedure of MIP/NPNi/GE was also monitored by CV in a probe solution. As shown in Figure 3a, compared with bare GE, the peak current of NPNi/GE was significantly enhanced, indicating that NPNi as an electrode modifier plays an important role in enhancing the sensor signal. By contrast, the peak currents of NPNi/GE covered with a poly(o-aminophenol) film containing MNZ dropped significantly. This can be explained by the fact that the polymer is not conductive, and after the whole electrode surface was densely wrapped with the polymeric film, there was essentially no channel for the active probe to access the electrode surface. This also demonstrates the successful decoration of a MIP thin film onto the entire surface of a NPNi-modified electrode. Extraction of the template MNZ was implemented by using 0.1 M NaOH, which could cause breakage of noncovalent interactions between the functional monomers and the template molecules.[23,24] After removal of the template from the polymeric network, some channels were created so that the probe ions could pass through the cavities to transfer onto the electrode surface, which is illustrated by amplification of the peak current values (Figure 3a). In order to demonstrate the binding ability of the sensor toward the template, the sensor was incubated in a solution containing MNZ, and the
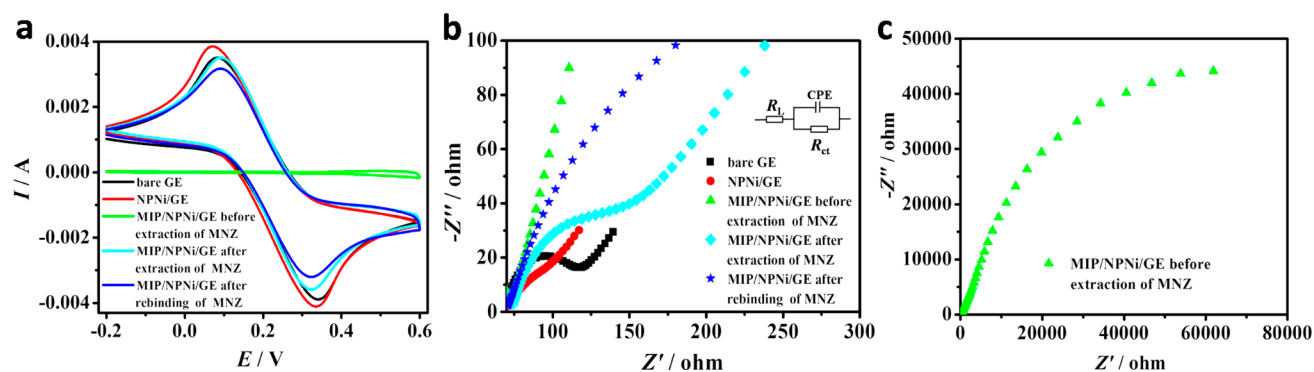
Figure 3. Cyclic voltammograms (a) and Nyquist diagrams of EIS (b) of different electrodes during the preparation process and the complete EIS curve of MIP/NPNi/GE before extraction of MNZ (c). The inset of part b is the equivalent circuit for the EIS test. The supporting solution of CV contained 0.1 M $Fe(CN)_6^{3-/4-}$ and 0.1 M KNO_3, and that of EIS contained 5 mM $Fe(CN)_6^{3-/4-}$ and 0.1 M KCl. The scan rate of CV was 100 mV s^{-1}, and the frequency range of EIS was from 0.01 Hz to 100 kHz.
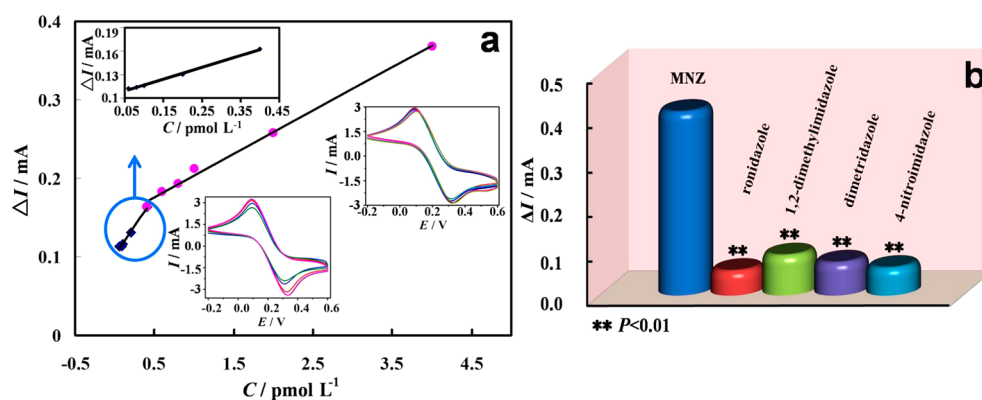
Figure 4. (a) Calibration curves for MNZ detection correlating the reduction peak current shift with the MNZ concentration by using MIP/NPNi/GE. The calibration curve in the top-left inset is obtained with the MNZ concentration in the range of 6×10^{-14}–4×10^{-13} M, and the cyclic voltammograms in accordance are in the bottom-left inset, while the bottom-right inset shows cyclic voltammograms with the MNZ concentration in the range of 4.0×10^{-13}–4×10^{-12} M. (b) Determination of MNZ and some of its structural analogues at the same concentration of 2×10^{-12} M by using MIP/NPNi/GE.

corresponding cyclic voltammogram was recorded. As shown in Figure 3a, after incubation, the peak current of the probe was diminished, which could be ascribed to blockage of the channels used for probe transfer due to the binding of template molecules with the MIP film. The subdued signal may be attributed to noncovalent interactions, including hydrogen bonds between the amino group of o-aminophenol and nitro groups and the nitrogen in the imidazole ring of MNZ, electrostatic force between the amino group of o-aminophenol and the hydroxyl of MNZ, and van der Waals force.

Electron impact spectroscopy (EIS) was used for further characterization of the modified electrode. Generally, the impedance spectra include a semicircle portion and a linear portion. The semicircle diameter at higher frequencies corresponds to electron-transfer resistance, and the linear part at lower frequencies is related to the diffusion process. It can be seen that a small well-defined semicircle was obtained at the bare GE, indicating small interface impedance (Figure 3b). Modification with NPNi caused the semicircle to almost disappear because of the excellent electroconductibility of NPNi. When MIP was deposited on the surface of NPNi/GE, the impedance values obviously increased, which could be a consequence of the compact and nonconductive MIP film introducing resistance into the electrode/solution interface. However, the interface electron resistance decreased remark-

ably after MNZ was removed, suggesting the successful formation of pores due to extraction of MNZ molecules. At last, rebinding of MNZ (1×10^{-12} M) with MIP/NPNi/GE led to an upward change of the impedance values, which could be explained by occupation of part of the imprinted sites by MNZ (Figure 3b).

The current shift of the cathodic reduction peak (ΔI) before and after binding with MNZ was calculated for evaluation of a sensor's response (Figure S2 in the SI). It is evident that the response of MIP/NPNi/GE is 2.09 times higher than that of MIP/GE (Figure S2a in the SI), revealing the signal enhancement effect from NPNi. It is assumed that the nanoporous structure of the electrodeposited 3D Ni layer provides a platform with a large surface area for loading the upper MIP film, raising the amount of imprinted sites and consequently boosting the sensitivity and binding capacity.

In addition, the responses of bare GE, NIP/GE, and MIP/GE to MNZ at the same concentration were also explored (Figure S2b in the SI). Imperceptible change in ΔI of bare GE and NIP/GE was observed, while MIP/GE displayed an obvious response toward MNZ, confirming that the existence of imprinted sites in the MIP film plays an important role in binding MNZ.

3.2. Calibration Curve and Detection Limit. The calibration curves of the current response versus MNZ

Table 1. Comparison of the Major Characteristics of Some Reported Methods Used in Detecting MNZ

electrode	dynamic range (nM)	LOD (nM)	RSD (%)	ref
Fe_3O_4/SiO_2-MIP/magnetic GCE[a]	$50-1 \times 10^3$	16	3.5	5
graphene-ionic/liquid/GCE[a]	$100-2.5 \times 10^4$	47	2.1	16
single-walled carbon nanotube/GCE[a]	$100-2 \times 10^5$	63		21
carbon fiber microdisk electrode	$1 \times 10^3 - 2.2 \times 10^4$	500	3.7	25
gold electrode	$1-2 \times 10^3$	0.1	1.84	18
MIP/carbon paste electrode	0. 33−450	0. 21	3.8	20
cysteic acid/PDDA-GN[b]/GCE[a]	$10-1 \times 10^3$	2.3	3.26	7
MWCNT[c]/MIP/GCE[a]	$1-1.2 \times 10^3$	0.287	0.6	24
NPGL[d]/MIP/GE	$0.05-1.4 \times 10^3$	0.018	0.8	23
MIP-modified pencil graphite electrode	$0.057-7.59 \times 10^5$	5.84×10^{-3}	1.8	15
Ni/Fe-layered double hydroxides/GCE[a]	$5 \times 10^3-1.61 \times 10^6$	5.8×10^3	<4.0	17
magnetic MIP/graphene/GCE[a]	$32-3.4 \times 10^3$	1.2	7.8	19
poly(chromotrope 2B)/GCE[a]	$1 \times 10^4-4 \times 10^5$	330	2.26	22
MIP/NPNi/GE	$6 \times 10^{-5}-4 \times 10^{-3}$	2×10^{-5}	1.12	this work

[a]GCE refers to glassy carbon electrode. [b]PDDA-GN refers to poly(diallyldimethylammonium chloride)-functionalized graphene. [c]MWCNT refers to multiwalled carbon nanotube. [d]NPGL refers to a nanoporous gold leaf.

concentration for MIP/NPNi/GE are shown in Figure 4a, the inset of which shows the corresponding cyclic voltammograms. Double linearity can be found where the peak currents are proportional to the concentration of MNZ in the ranges of $6 \times 10^{-14}-4 \times 10^{-13}$ M and $4 \times 10^{-13}-4 \times 10^{-12}$ M with a detection limit of 2×10^{-14} M at a signal-to-noise ratio of 3. The comparison of our sensor with other reported sensors in determining MNZ is summarized in Table 1, which shows that the as-prepared sensor has the lowest detection limit compared with its counterparts.

The existence of double linear ranges could originate from the different affinity levels and the nonuniform distribution of imprinted sites in the MIP film. Specifically, when MNZ is at low concentration, they prefer to occupy the imprinted sites of high affinity and located at the surface of the MIP film. Then, the presence of more MNZ molecules may lead the low-affinity sites residing in a deeper polymeric skeleton to begin binding the templates, showing a decreased slope in the linear regression equation.

Useful information involving the electrochemical mechanism usually can be acquired by investigating the effect of the scan rate on the peak current (Figure S3 in the SI). It is observed that the reduction peak currents increased linearly with the square root of the scan rates in the range of 10−150 mV s^{-1}, with two linear regression equations of $I_{cp} = 0.000034v^{1/2} - 0.000076$ ($R^2 = 0.9949$) and $I_{ap} = -0.000037v^{1/2} + 0.000091$ ($R^2 = 0.9935$). This indicates that the recognition of MNZ upon the developed sensor is a diffusion-controlled process, which is the ideal case for quantitative determination.[49]

3.3. Repeatability and Stability. The repeatability of the sensor was evaluated by measuring three levels of MNZ solution (2×10^{-13}, 4×10^{-13}, and 6×10^{-13} M) for three successive times with the same modified electrode. The results reveal that the electrode possesses a satisfying repeatability with a relative standard deviation (RSD) of less than 1.12%, suggesting that the developed method is suitable for the routine quality control analysis of the drug in pharmaceutical dosage and biological fluids. The stability of the modified electrode was also examined by using the same electrode for repetitive analysis of MNZ (4×10^{-13} M) in 30 days, brought out with a RSD of 1.4%. Moreover, the sensor retains a response of 96.6% of the initial current after 30 days of storage in a desiccator at room temperature.

3.4. Selectivity. The selectivity was investigated by testing the structural analogues of MNZ, including ronidazole, 4-nitroimidazole, 1,2-dimethylimidazole, and dimetridazole, the chemical structures of which are displayed in Figure S4 in the SI. It is found that the current response of MIP/NPNi/GE toward MNZ is much higher than that induced by the analogues at the same concentration (Figure 4b). The high specificity could be accredited to the complementary cavities in the polymeric matrix, which match the unique molecular structure of MNZ sterically and via multiple interactions between functional groups in the polymer and template.

In order to further validate the specificity of the sensor, its current response was tested in a solution containing 6×10^{-13} M MNZ and a 10-fold amount of starch, sucrose, and dextrin, regarded as the major interfering molecules in the MNZ tablet, and glucose, Ca^{2+}, NH_4^+, Na^+, K^+, Cl^-, and NO_3^-, as the main interferents in biological sample (e.g., fish tissue). Compared with MNZ alone, the mixtures of MNZ and coexisting substances in tablet and biosample give responses of 99.1% and 102.7%, respectively, reflecting the excellent interference resistibility of the constructed sensor.

3.5. Real Sample Analysis. The practical utility of the sensor was surveyed by determining the concentration of MNZ in pharmaceutical drug and fish tissue using the standard addition method. Recovery was calculated by dividing the difference between the detected quantity of MNZ in spiked and nonspiked samples by the quantity of MNZ spiked. The recoveries of the samples are 91.3−112.5% and 91.9−100.7% for tablet (Table 2) and fish tissue (Table 3), respectively, indicating the good accuracy and repeatability of the developed

Table 2. Determination of MNZ in Tablet Using MIP/NPNi/GE ($n = 3$)[a]

theory value of sample ($\times 10^{-13}$ M)	spiked ($\times 10^{-13}$ M)	measurement value of sample ($\times 10^{-13}$ M)	measurement value of total ($\times 10^{-12}$M)	recovery (%)	RSD (%)
5.84		5.33 ± 0.12		91.3	2.3
5.84	4.67	5.33 ± 0.12	1.05 ± 0.013	110.7	1.2
5.84	5.84	5.33 ± 0.12	1.19 ± 0.054	112.5	4.5
5.84	7.01	5.33 ± 0.12	1.27 ± 0.028	105.1	2.2

[a]Mean ± standard deviation.

Table 3. Determination of MNZ in Fish Tissue Using MIP/NPNi/GE ($n = 3$)[a]

measurement value of sample ($\times 10^{-13}$ M)	spiked ($\times 10^{-13}$ M)	measurement value of total ($\times 10^{-13}$ M)	recovery (%)	RSD (%)
4.62				
4.62	3.70	8.02 ± 0.43	91.9	5.4
4.62	4.62	9.12 ± 0.29	97.4	3.2
4.62	5.54	10.2 ± 0.37	100.7	3.6

[a]Mean ± standard deviation.

method in real sample analysis. In order to further demonstrate the accuracy and reliability of the sensing system, assay of the tablet sample was carried out by using the presented sensor and HPLC (as a standard method). Table S1 in the SI illustrates a superb agreement between the data obtained by our proposed methodology and the HPLC reference approach with the same sample. The *t*-test shows that there is no significant difference between them at a confidence level of 99%.

4. CONCLUSION

In this work, a sensitive and selective electrochemical sensing protocol based on MIP/NPNi nanocomposites was developed as an attractive alternative for MNZ assessment. The unique porous structure and good conductivity of NPNi allows it to serve as a great platform for loading the outer imprinted film for recognizing the molecules of interest. Comparison between the present method and the previous reports for MNZ determination by sensing approach reveals that our hybrid sensor shows excellent performance in terms of ultralow detection limit, high selectivity, and good repeatability over other sensors. The superior merits of the as-obtained sensing architecture are summarized as follows: (1) The 3D NPNi framework provides an enlarged highly conductive surface area and easier diffusion of electron transfer. (2) Selectivity is guaranteed by the specific identification ability of an electropolymerized MIP film. (3) The facile electrochemical deposition method and cost-effectiveness benefit its practicability. Above all, the synergetic tactic coupling NPNi with MIP could be an extremely promising route for a broad range of electrochemical chem/biosensing applications.

■ ASSOCIATED CONTENT

ⓢ Supporting Information
Cyclic voltammograms for the electrochemical polymerization of MNZ/MIP (Figure S1), CV responses of differently modified electrodes toward MNZ at the same concentration (Figure S2), influence of the scan rate on the response of MIP/NPNi/GE toward MNZ (Figure S3), chemical structures of MNZ and its structural analogues (Figure S4), and comparison for determination of MNZ in tablet by using HPLC and the modified sensor (Table S1). The Supporting Information is available free of charge on the ACS Publications website at DOI: 10.1021/acsami.5b03755.

■ AUTHOR INFORMATION

Corresponding Authors
*Tel: +86-993-2057005. E-mail: yingchunli@shzu.edu.cn.
*Tel: +86-991-88366513. E-mail: sunzhipengxj@gmail.com.
Notes
The authors declare no competing financial interest.

■ REFERENCES

(1) Freeman, C. D.; Klutman, N. E.; Lamp, K. C. *Drugs* **1997**, *54*, 679−708.
(2) Muller, J.; Schildknecht, P.; Muller, N. Metabolism of Nitro Drugs Metronidazole and Nitazoxanide in Giardia Lamblia: Characterization of A Novel Nitroreductase (GlNR2). *J. Antimicrob. Chemother.* **2013**, *68*, 1781−1789.
(3) Abbaspoor, Z.; Rabee, Z.; Najjar, S. Efficacy and Safety of Oral Tinidazole and Metronidazole in Treatment of Bacterial Vaginosis: A Randomized Control trial. *Pharmacol. Res.* **2014**, *4*, 78−83.
(4) Bucklin, M. H.; Groth, C. M.; Henriksen, B. *Encyclopedia of Toxicology*, 3rd ed.; Academic Press: Salt Lake City, UT, 2014; pp 330 and 331.
(5) Chen, D.; Deng, J.; Liang, J.; Xie, J.; Hu, C.; Huang, K. A Core-Shell Molecularly Imprinted Polymer Grafted onto A Magnetic Glassy Carbon Electrode as A Selective Sensor for the Determination of Metronidazole. *Sens. Actuators, B* **2013**, *183*, 594−600.
(6) Han, J.; Zhang, L.; Yang, S.; Wang, J.; Tan, D. Detrimental Effects of Metronidazole on Selected Innate Immunological Indicators in Common Carp (Cyprinus Carpio L.). *Bull. Environ. Contam. Toxicol.* **2014**, *92*, 196−201.
(7) Liu, W.; Zhang, J.; Li, C.; Tang, L.; Zhang, Z.; Yang, M. A Novel Composite Film Derived From Cysteic Acid and PDDA-Functionalized Graphene: Enhanced Wensing Material for Electrochemical Determination of Metronidazole. *Talanta* **2013**, *104*, 204−211.
(8) U.S. Food and Drug Administration. Prohibited and Restricted Drugs in Food Animals From Food Animal Residue Avoidance Databank. Regulatory information. Available at http://www.farad.org/eldu/prohibit.asp (accessed March 6, 2015).
(9) International Agency for Research on Cancer of World Health Organization. Agents Classified by the IARC Monographs. List of Classifications, Available at http://monographs.iarc.fr/ENG/Classification/index.php (accessed March 2, 2015).
(10) Fabayo, A. B.; Grudzinski, S. K. Quality Control of Drugs. III. Quantitative Determination of Metronidazole in Tablets by UV-absorption Spectrophotometry. *Acta Polym. Pharm.* **1985**, *42*, 49−54.
(11) Tan, S. Z.; Jiang, J. H.; Yan, B. N.; Shen, G. L.; Yu, R. Q. Preparation of A Novel Fluorescence Probe Based on Covalent Immobilization by Emulsion Polymerization and Its Application to the Determination of Metronidazole. *Anal. Chim. Acta* **2006**, *560*, 191−196.
(12) Ali, N. W.; Gamal, M.; Abdelkawy, M. Chromatographic Methods for Simultaneous Determination of Diiodohydroxyquinoline and Metronidazole in their Binary Mixture. *Pak. J. Pharm. Sci.* **2013**, *26*, 865−871.
(13) Wang, J. H. Determination of Three Nitroimidazole Residues in Poultry Meat by Gas Chromatography with Nitrogen-phosphorus Detection. *J. Chromatogr. A* **2001**, *918*, 435−438.
(14) Trivedi, K. D.; Chaudhary, A. B.; Mohan, S. Development and Validation of RP-HPLC Method for Estimation of Metronidazole and Norfloxacin in Suspension Form. *Int. J. Adv. Pharm.* **2013**, *2*, 5−11.
(15) Roy, E.; Maity, S. K.; Patra, S.; Madhuri, R.; Sharma, P. K. Ametronidazole-probe Sensor Based on Imprinted Biocompatible Nanofilm for Rapid and Sensitive Detection of Anaerobic Protozoan. *RSC Adv.* **2014**, *4*, 32881−32893.

(16) Peng, J.; Hou, C.; Hu, X. Determination of Metronidazole in Pharmaceutical Dosage Forms Based on Reduction at Graphene and Ionic Liquid Composite Film Modified Electrode. *Sens. Actuators, B* **2012**, *169*, 81−87.

(17) Nejati, K.; Asadpour-Zeynali, K. Electrochemical Synthesis of Nickel-iron Layered Double Hydroxide: Application as A Novel Modified Electrode in Electrocatalytic Reduction of Metronidazole. *Mater. Sci. Eng., C* **2014**, *35*, 179−184.

(18) Mollamahale, Y. B.; Ghorbani, M.; Ghalkhani, M.; Vossoughi, M.; Dolati, A. Highly Sensitive 3D Gold Nanotube Ensembles: Application to Electrochemical Determination of Metronidazole. *Electrochim. Acta* **2013**, *106*, 288−292.

(19) Yang, G.; Zhao, F.; Zeng, B. Magnetic Entrapment for Fast and Sensitive Determination of Metronidazole with A Novel Magnet-controlled Glassy Carbon Electrode. *Electrochim. Acta* **2014**, *135*, 154−160.

(20) Gholivand, M. B.; Torkashvand, M. A Novel High Selective and Sensitive Metronidazole Voltammetric Sensor Based on A Molecularly Imprinted Polymer-carbon Paste Electrode. *Talanta* **2011**, *84*, 905−912.

(21) Salimi, A.; Izadi, M.; Hallaj, R.; Rashidi, M. Simultaneous Determination of Ranitidine and Metronidazole at Glassy Carbon Electrode Modified with Single Wall Carbon Nanotubes. *Electroanalysis* **2007**, *19*, 1668−1676.

(22) Li, X.; Xu, G. Simultaneous Determination of Ranitidine and Metronidazole in Pharmaceutical Formulations at Poly(chromotrope 2B) Modified Activated Glassy Carbon Electrodes. *J. Food Drug Anal.* **2014**, *22*, 345−349.

(23) Li, Y.; Liu, Y.; Liu, J.; Liu, J.; Tang, H.; Cao, C.; Zhao, D.; Ding, Y. Molecularly Imprinted Polymer Decorated Nanoporous Gold for Highly Selective and Sensitive Electrochemical Sensors. *Sci. Rep.* **2015**, *5*, 7699−7706.

(24) Liu, Y.; Liu, J.; Tang, H.; Liu, J.; Xu, B.; Yu, F.; Li, Y. Fabrication of Highly Sensitive and Selective Electrochemical Sensor by Using Optimized Molecularly Imprinted Polymers on Multi-walled Carbon Nanotubes for Metronidazole Measurement. *Sens. Actuators, B* **2015**, *206*, 647−652.

(25) Bartlett, P. N.; Ghoneim, E.; El-Hefnawy, G.; El-Hallag, I. Voltammetry and Determination of Metronidazole at A Carbon Fiber Microdisk Electrode. *Talanta* **2005**, *66*, 869−874.

(26) Xie, C.; Gao, S.; Guo, Q.; Xu, K. Electrochemical Sensor for 2,4-dichlorophenoxy Acetic Acid Using Molecularly Imprinted Polypyrrole Membrane as Recognition Element. *Microchim. Acta* **2010**, *169*, 145−152.

(27) Arvand, M.; Alirezanejad, F. New Sensing Material of Molecularly Imprinted Polymer for the Selective Recognition of Sulfamethoxazole in Foods and Plasma and Employing the Taguchi Optimization Methodology to Optimize the Carbon Paste Electrode. *J. Iran. Chem. Soc.* **2013**, *10*, 93−105.

(28) Li, Y.; Fu, Q.; Zhang, Q.; He, L. Preparation and Evaluation of Uniform-size (−)-Ephedrine-imprinted Polymeric Microspheres by Multi-step Swelling and Suspension Polymerization. *Anal. Sci.* **2006**, *22*, 1355−1360.

(29) Lin, L.; Li, Y.; Fu, Q.; He, L.; Zhang, J.; Zhang, Q. Preparation of Molecularly Imprinted Polymer for Sinomenine and Study on Its Molecular Recognition Mechanism. *Polymer* **2006**, *47*, 3792−3798.

(30) Mayes, A. G.; Mosbach, K. Molecularly Imprinted Polymers: Useful Materials for Analytical Chemistry? *TrAC, Trends Anal. Chem.* **1997**, *16*, 321−332.

(31) Liu, J.; Song, H.; Liu, J.; Liu, Y.; Li, L.; Tang, H.; Li, Y. Preparation of Molecularly Imprinted Polymer with Double Templates for Rapid Simultaneous Determination of Melamine and Dicyandiamide in Dairy Products. *Talanta* **2015**, *134*, 761−767.

(32) Liu, J.; Zhang, L.; Song, L. L. H.; Liu, Y.; Tang, H.; Li, Y. Synthesis of Metronidazole-imprinted Molecularly Imprinted Polymers by Distillation Precipitation Polymerization and Their Use as A Solid-phase Adsorbent and Chromatographic Filler. *J. Sep. Sci.* **2015**, *38*, 1172−1178.

(33) Haginaka, J. Molecularly Imprinted Polymers as Affinity-based Separation Media for Sample Preparation. *J. Sep. Sci.* **2009**, *32*, 1548−1565.

(34) Wu, W.; Shen, J.; Li, Y.; Zhu, H.; Banerjee, P.; Zhou, S. Specific Glucose-to-SPR Signal Transduction at Physiological pH by Molecularly Imprinted Responsive Hybrid Microgels. *Biomaterials* **2012**, *33*, 7115−7125.

(35) Bala, A.; Pietrzak, M.; Zajda, J.; Malinowska, E. Further Studies on Application of Al(III)-tetraazaporphine in Membrane-based Electrochemical Sensors for Determination of Fluoride. *Sens. Actuators, B* **2015**, *207*, 1004−1009.

(36) Wang, M.; Gao, Y.; Sun, Q.; Zhao, J. Ultrasensitive and Simultaneous Determination of the Isomers of Amaranth and Ponceau 4R in Foods Based on New Carbon Nanotube/polypyrrole Composites. *Food Chem.* **2015**, *172*, 873−879.

(37) Cui, G.; Zhang, M.; Zou, G. Resonant Tunneling Modulation in Quasi-2D Cu_2O/SnO_2 *p-n* Horizontal-multi-layer Heterostructure for Room Temperature H_2S Sensor Application. *Sci. Rep.* **2013**, *3*, 1250.

(38) Jiang, D.; Zhang, Y.; Chu, H.; Liu, J.; Wan, J.; Chen, M. N-doped Graphene Quantum Dots as An Effective Photocatalyst for the Photochemical Synthesis of Silver Deposited Porous Graphitic C_3N_4 Nanocomposites for Nonenzymatic Electrochemical H_2O_2 Sensing. *RSC Adv.* **2014**, *4*, 16163−16171.

(39) Ananthi, A.; Kumar, S. S.; Phani, K. L. Facile One-step Direct Electrodeposition of Bismuth Nanowires on Glassy Carbon Electrode for Selective Determination of Folic Acid. *Electrochim. Acta* **2015**, *151*, 584−590.

(40) Wang, J.; Gao, H.; Sun, F.; Xu, C. Nanoporous PtAu Alloy as An Electrochemical Sensor for Glucose and Hydrogen Peroxide. *Sens. Actuators, B* **2014**, *191*, 612−618.

(41) Fan, H.; Guo, Z.; Gao, L.; Zhang, Y.; Fan, D.; Ji, G.; Du, B.; Wei, Q. Ultrasensitive Electrochemical Immunosensor for Carbohydrate Antigen 72−4 Based on Dual Signal Amplification Strategy of Nanoporous Gold and Polyaniline-Au Asymmetric Multicomponent Nanoparticles. *Biosens. Bioelectron.* **2015**, *64*, 51−56.

(42) Chang, J. K.; Wu, C. M.; Sun, I. W. Nano-architectured $Co(OH)_2$ Electrodes Constructed Using An Easily-manipulated Electrochemical Protocol for High-performance Energy Storage Applications. *J. Mater. Chem.* **2010**, *20*, 3729−3735.

(43) Lu, W.; Qin, X.; Asiri, A. M.; Al-Youbi, A. O.; Sun, X. Ni Foam: A Novel Three-dimensional Porous Sensing Platform for Sensitive and Selective Nonenzymatic Glucose Detection. *Analyst* **2013**, *138*, 417−420.

(44) Shervedani, R. K.; Karevan, M.; Amini, A. Prickly Nickel Nanowires Grown on Cu Substrate as A Supersensitive Enzyme-free Electrochemical Glucose Sensor. *Sens. Actuators, B* **2014**, *204*, 783−790.

(45) Liu, B.; Luo, L.; Ding, Y.; Si, X.; Wei, Y.; Ouyang, X.; Xu, D. Differential Pulse Voltammetric Determination of Ascorbic Acid in the Presence of Folic Acid at Electro-deposited NiO/graphene Composite Film Modified Electrode. *Electrochim. Acta* **2014**, *142*, 336−342.

(46) Li, L.; Liu, M.; He, S.; Chen, W. Freestanding 3D Mesoporous Co_3O_4@Carbon Foam Nanostructures for Ethanol Gas Sensing. *Anal. Chem.* **2014**, *86*, 7996−8002.

(47) Li, C.; Kurniawan, M.; Sun, D.; Tabata, H.; Delaunay, J. J. Nanoporous CuO Layer Modified Cu Electrode for High Performance Enzymatic and Non-enzymatic Glucose Sensing. *Nanotechnology* **2015**, *26*, 15503.

(48) Noroozifar, M.; Khorasani-Motlagh, M.; Hassani Nadiki, H.; Saeed Hadavi, M.; Mehdi Foroughi, M. Modified Fluorine-doped Tin Oxide Electrode with Inorganic Ruthenium Red Dye-multiwalled Carbon Nanotubes for Simultaneous Determination of Dopamine, Uric Acid, and Tryptophan. *Sens. Actuators, B* **2014**, *204*, 333−341.

(49) Dong, X.; Ma, Y.; Zhu, G.; Huang, Y.; Wang, J.; Chan-Park, M. B.; Wang, L.; Huang, W.; Chen, P. Synthesis of Graphene-carbon Nanotube Hybrid Foam and Its Use as A Novel Three-dimensional Electrode for Electrochemical Sensing. *J. Mater. Chem.* **2012**, *22*, 17044−17048.